

## SUPPLEMENTARY INFORMATION

### Microhexagon gradient array directs spatial diversification of spinal motor neurons

Geok Soon Lim<sup>1,2,#</sup>, Jin Hui Hor<sup>2,3,#</sup>, Nicholas R.Y. Ho<sup>1,2</sup>, Chi Yan Wong<sup>1,2</sup>, Shi Yan Ng<sup>2,4,5,6</sup>, Boon Seng Soh<sup>2,3,6,\*</sup>, Huilin Shao<sup>1,2,5,7,8,\*</sup>

<sup>1</sup> Biomedical Institute for Global Health Research and Technology, National University of Singapore, 117599, Singapore

<sup>2</sup> Institute of Molecular and Cell Biology, Agency for Science, Technology and Research, 138673, Singapore

<sup>3</sup> Department of Biological Sciences, Faculty of Science, National University of Singapore, 117543, Singapore

<sup>4</sup> Department of Physiology, Yong Loo Lin School of Medicine, National University of Singapore, 117456, Singapore

<sup>5</sup> National Neuroscience Institute, 308433, Singapore

<sup>6</sup> Key Laboratory for Major Obstetric Diseases of Guangdong Province, The Third Affiliated Hospital of Guangzhou Medical University, Guangzhou, 510150, China

<sup>7</sup> Department of Biomedical Engineering, Faculty of Engineering, National University of Singapore, 117583, Singapore

<sup>8</sup> Department of Surgery, Yong Loo Lin School of Medicine, National University of Singapore, 119228, Singapore

# These authors contributed equally

\* Corresponding authors

Boon Seng Soh, PhD  
Institute of Molecular and Cell Biology  
61 Biopolis Drive Proteos  
#05-07, Singapore 138673  
(65) 6586 9530  
[bssoh@imcb.a-star.edu.sg](mailto:bssoh@imcb.a-star.edu.sg)

Huilin Shao, PhD  
National University of Singapore  
MD6, 14 Medical Drive  
#14-01, Singapore 117599  
(65) 6601 5885  
[huilin.shao@nus.edu.sg](mailto:huilin.shao@nus.edu.sg)

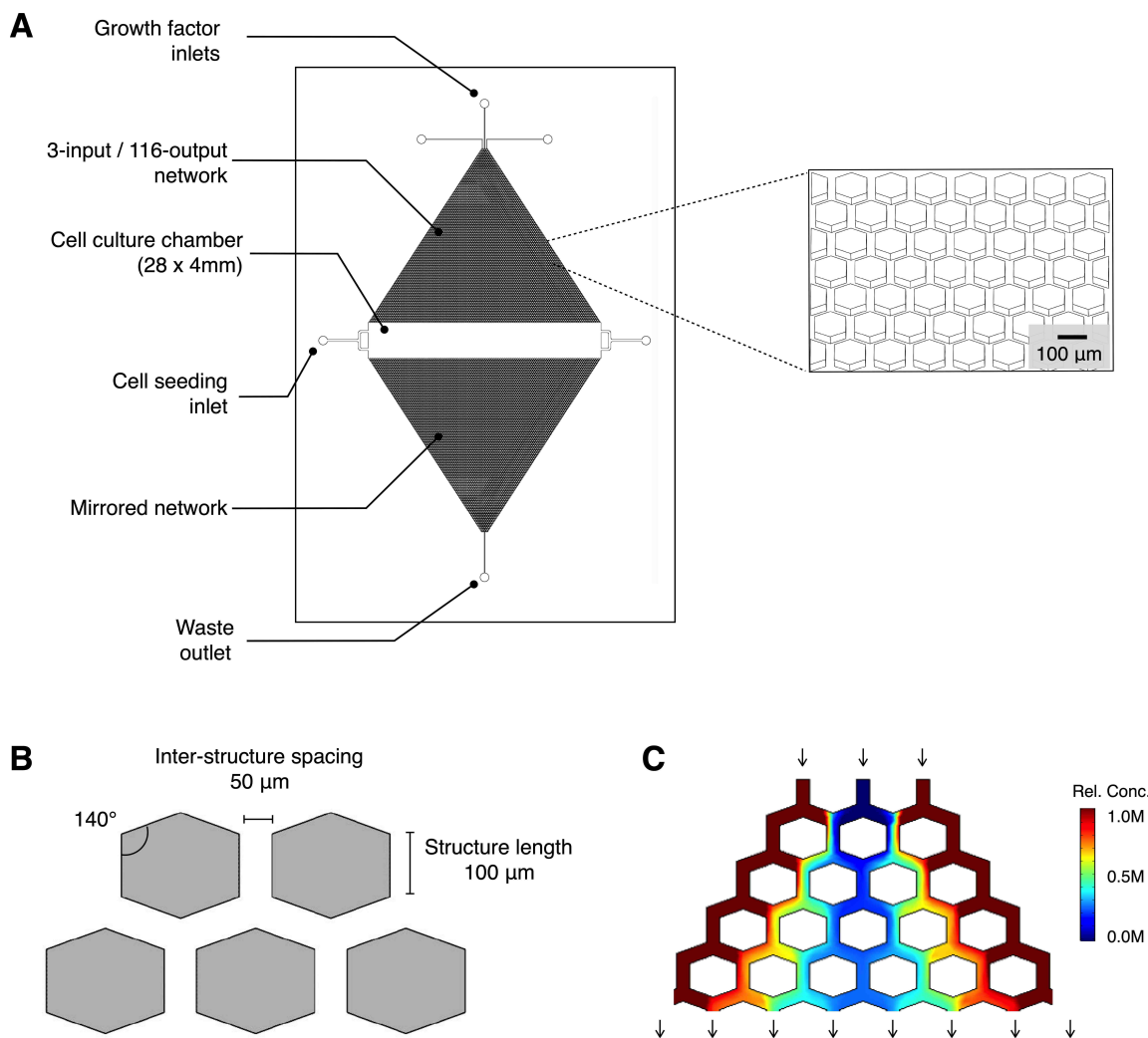


**Figure S1. Schematic illustration of the microHIVE platform.**

**(A)** The microHIVE platform consists of three growth factor inlets, a high-density divergent array of interlocking microhexagons (insert), an all-polymer cell culture chamber, and a mirrored network of microstructures connected to a single waste outlet. **(B)** Optimized structure length, internal angle and inter-structure spacing of the microhexagons to improve the array's lateral resolution in generating complex gradient profiles. **(C)** Simulation to illustrate fluid branching and mixing around of the microhexagon structures in generating high resolution concentration gradients.

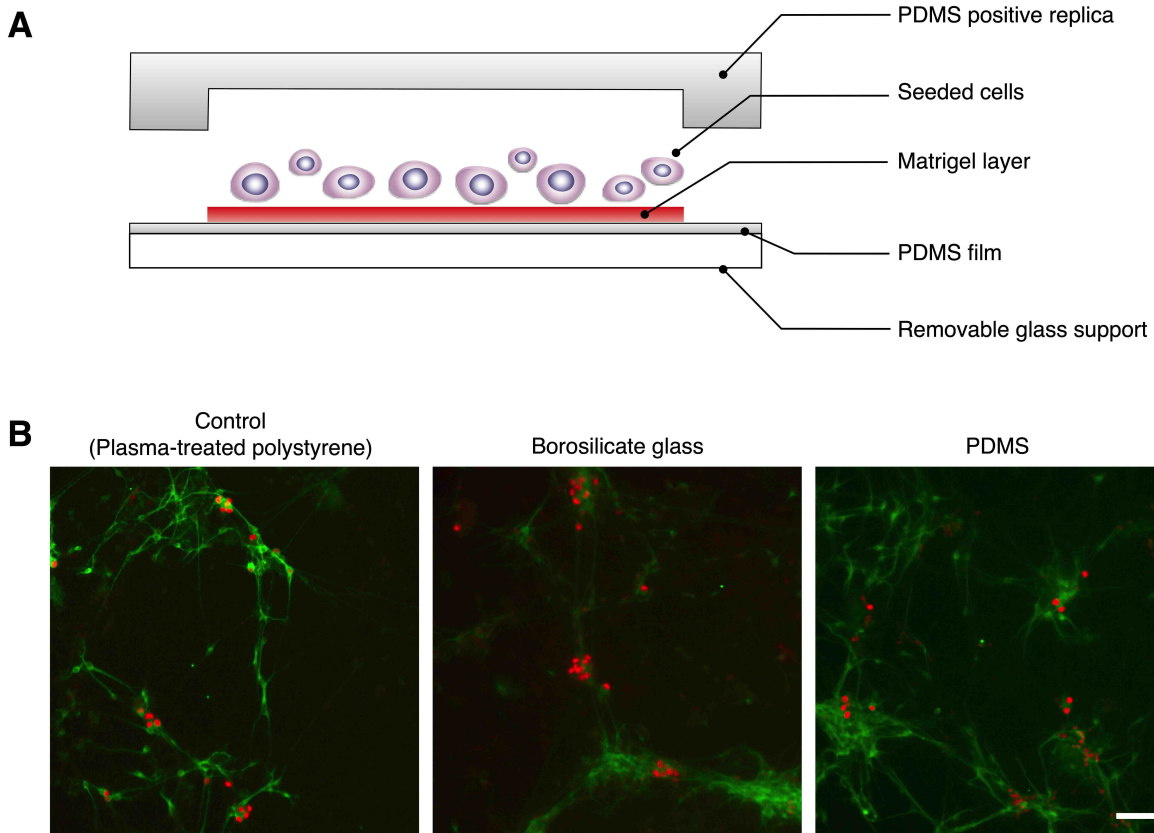


**Figure S2. Soft polymeric substrate for the cell culture chamber.**

**(A)** Cross-sectional schematic illustration of the cell culture chamber. The culture chamber is constructed primarily with soft polymer (PDMS) to enable easy sectioning. The bottom PDMS film is coated with a matrigel layer to promote cellular adhesion. The entire chamber is supported on a removable borosilicate glass. **(B)** Induced pluripotent stem cells (iPSC) were seeded on different substrates (i.e., polystyrene, glass and PDMS) and subjected to motor neuron differentiation. All substrates were coated with matrigel to promote cell adhesion. Co-staining of the differentiated cells for ISL1 (red, motor neuron marker) and MAP2 (green, microtubule control marker) showed good cellular proliferation and differentiation on the PDMS substrate, comparable to that of the gold-standard control. Scale bar indicates 100  $\mu$ m.

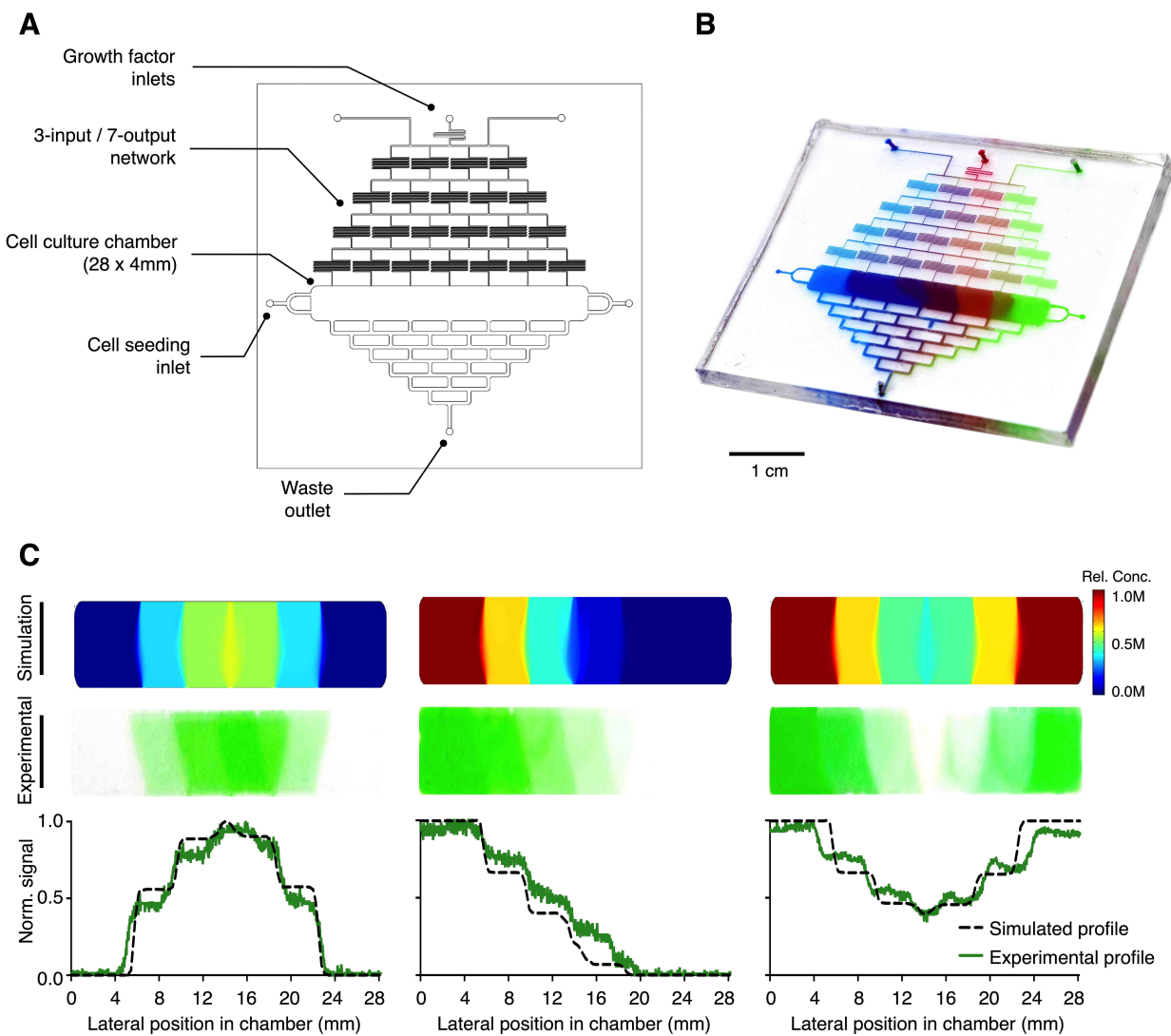


**Figure S3. Conventional concentration gradient generator.**

**(A)** Schematic illustration of the “Christmas-tree” gradient generator. The device consists of three inlets and a network of serpentine mixers that opens into a cell culture chamber of identical dimensions to that of the microHIVE platform. The device was designed to occupy the same footprint as the microHIVE platform. **(B)** Photograph of the “Christmas-tree” gradient generator with three different colored dyes. Note the discrete color changes in the resultant gradient. **(C)** Using the “Christmas-tree” gradient generator, we prepared the gradient profiles illustrated in Figure 2C. We first performed numerical simulations (top) and experimentally generated the profiles using colored dyes (middle). Quantitative correlation of the simulated and experimental profiles (bottom) showed reduced lateral resolution and step-wise nature of the gradients generated.

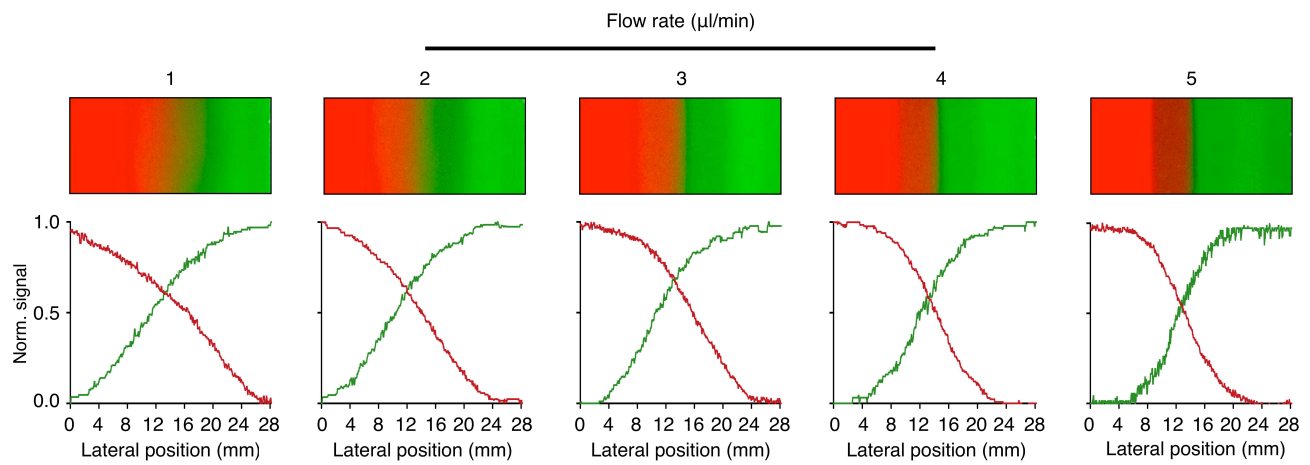


**Figure S4. Generation of simultaneous gradients with colored dyes.**

Generation of simultaneous gradients using red and green colored dyes, with increasing flow rates from 1  $\mu\text{l}/\text{min}$  to 5  $\mu\text{l}/\text{min}$ . The profile changes were de-convoluted and quantified through image analysis.

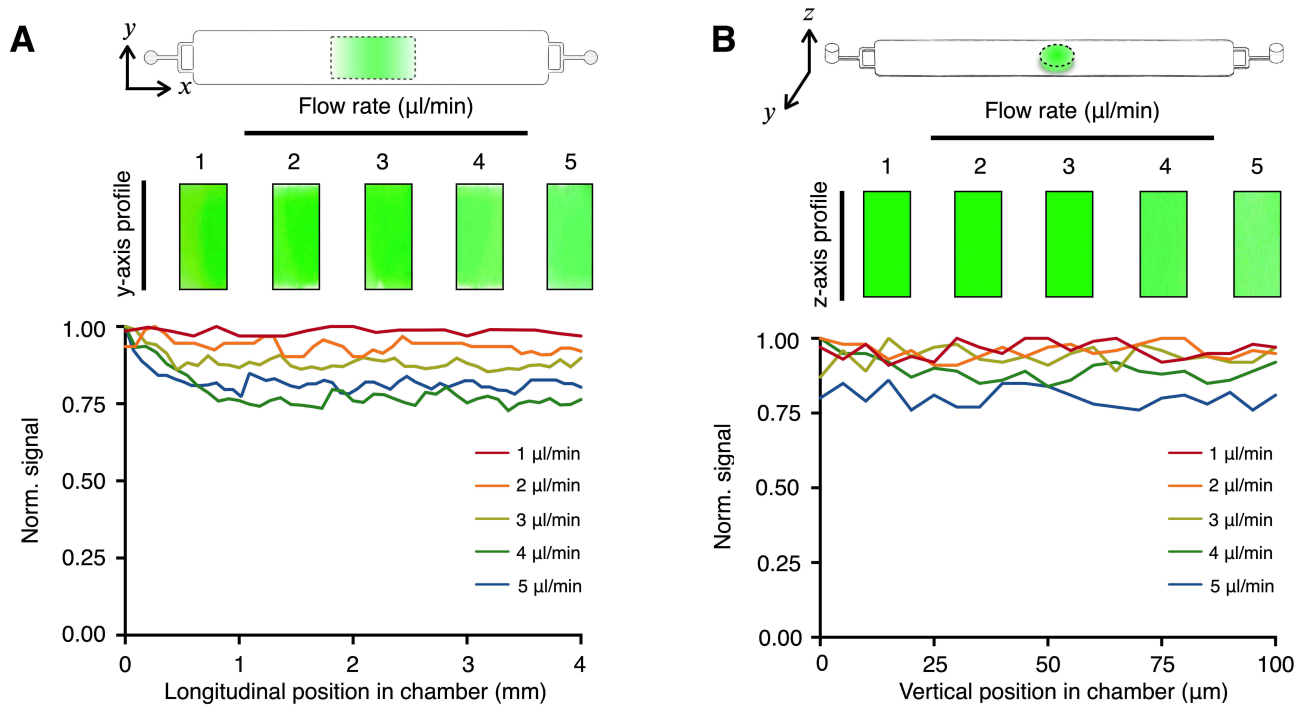


**Figure S5. Cross-sectional uniformity of molecular profiles in the cell culture chamber.**

The mirrored network connecting to the waste outlet helped to stabilize the concentration profile along the **(A)** y-axis (i.e., width) and **(B)** z-axis (i.e., depth) of the cell culture chamber, over a range of flow rates from 1  $\mu\text{l}/\text{min}$  to 5  $\mu\text{l}/\text{min}$ .

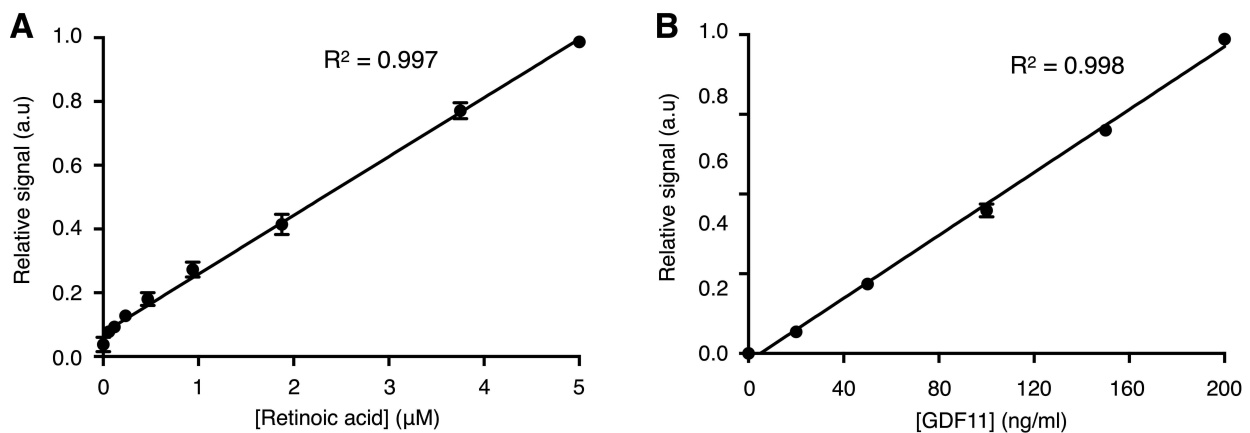


**Figure S6. Spectrometric measurements of retinoic acid and GDF11.**

Calibration curves of **(A)** retinoic acid and **(B)** GDF11. All measurements were performed through spectrometric absorbance measurements on known concentrations of the growth factors.

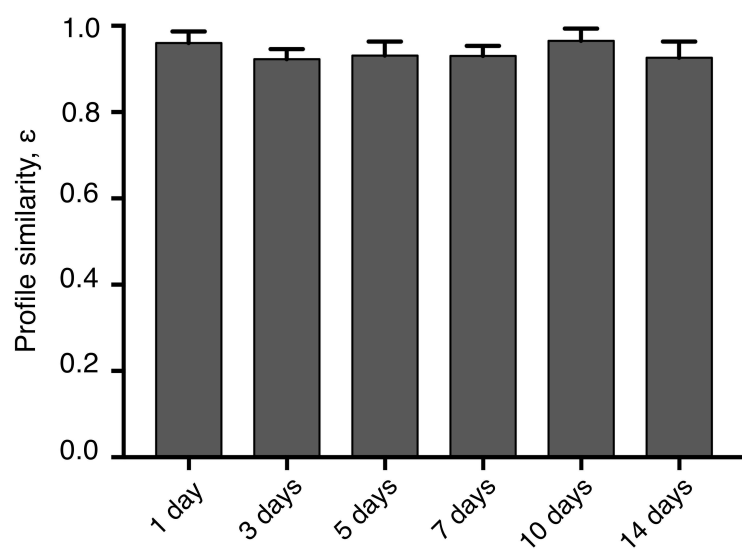


**Figure S7. Long-term maintenance of steady-state molecular profiles.**

The profile similarity metric  $\varepsilon$  was used to quantitatively analyze the robustness of the microHIVE platform in maintaining the desired molecular profile for 14 days.

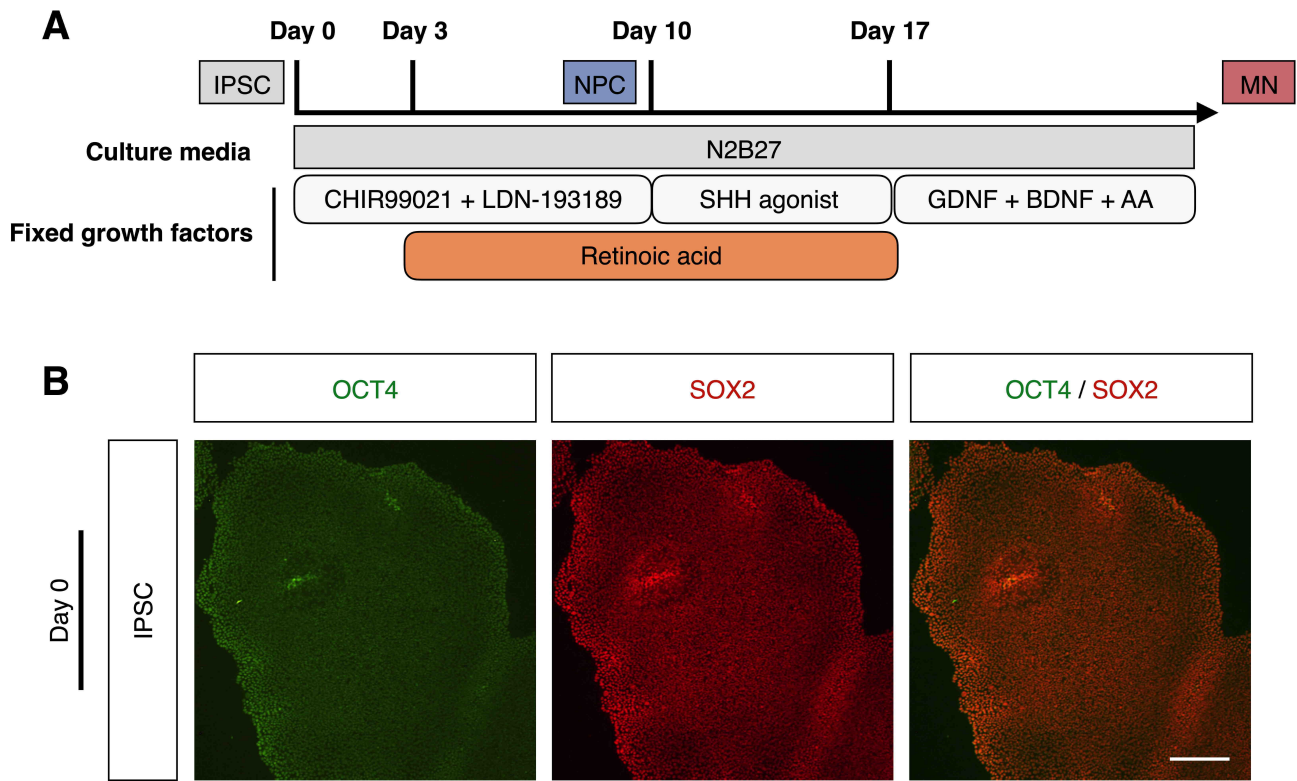


**Figure S8. Conventional motor neuron differentiation protocol.**

**(A)** Schematic illustration of conventional motor neuron differentiation from induced pluripotent stem cells (iPSC). Note that retinoic acid is added a fixed concentration ( $1.0 \mu\text{M}$ ) and no GDF11 is included in the protocol. **(B)** Co-staining of OCT4 (green) and SOX2 (red) showed that the iPSC maintained pluripotency before differentiation into spinal motor neurons. Scale bar indicates  $100 \mu\text{m}$ .

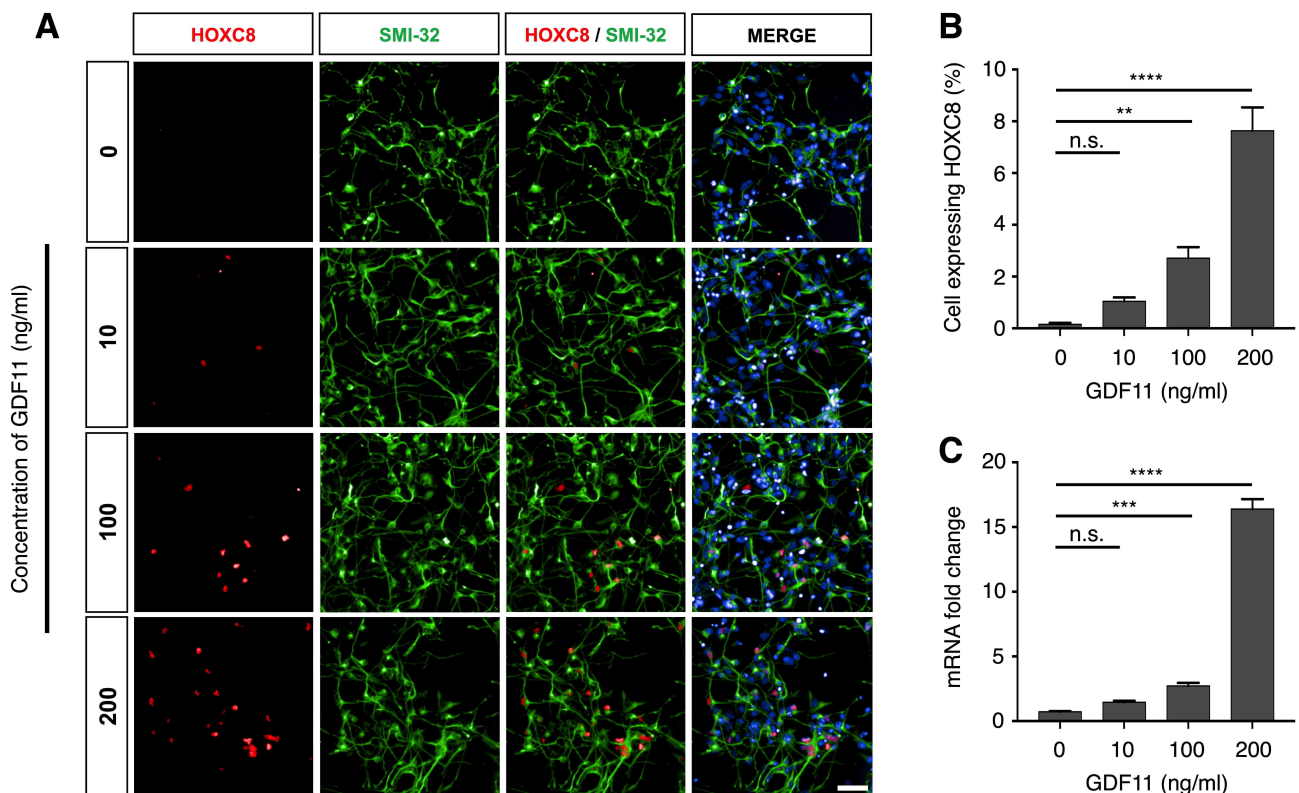


**Figure S9. Addition of GDF11 generates thoracic motor neurons.**

**(A)** Varying concentrations of GDF11 (0 – 200 ng/ml), in the presence of fixed concentration of retinoic acid (1  $\mu$ M), were used to generate spinal motor neurons. Immunostaining with HOXC8 (red) and SMI-32 (green) at day 28 indicated successful generation of thoracic motor neurons. Cellular nuclei were counterstained with DAPI. Scale bar indicates 50  $\mu$ m. **(B)** Cellular quantification based on positive immunostaining of HOXC8 showed increasing cell counts when cells were treated with elevated concentrations of GDF11. **(C)** Quantitative PCR analysis showed up-regulation of HOXC8 mRNA transcript with increasing GDF11 treatment, consistent with the protein expression trend identified by immunofluorescence staining. All mRNA analyses were normalized against that of cells treated with no GDF11 (i.e., 0 ng/ml). (\*\*  $P < 0.01$ , \*\*\*  $P < 0.001$ , \*\*\*\*  $P < 0.0001$ , n.s. not significant, Student's *t*-test.)

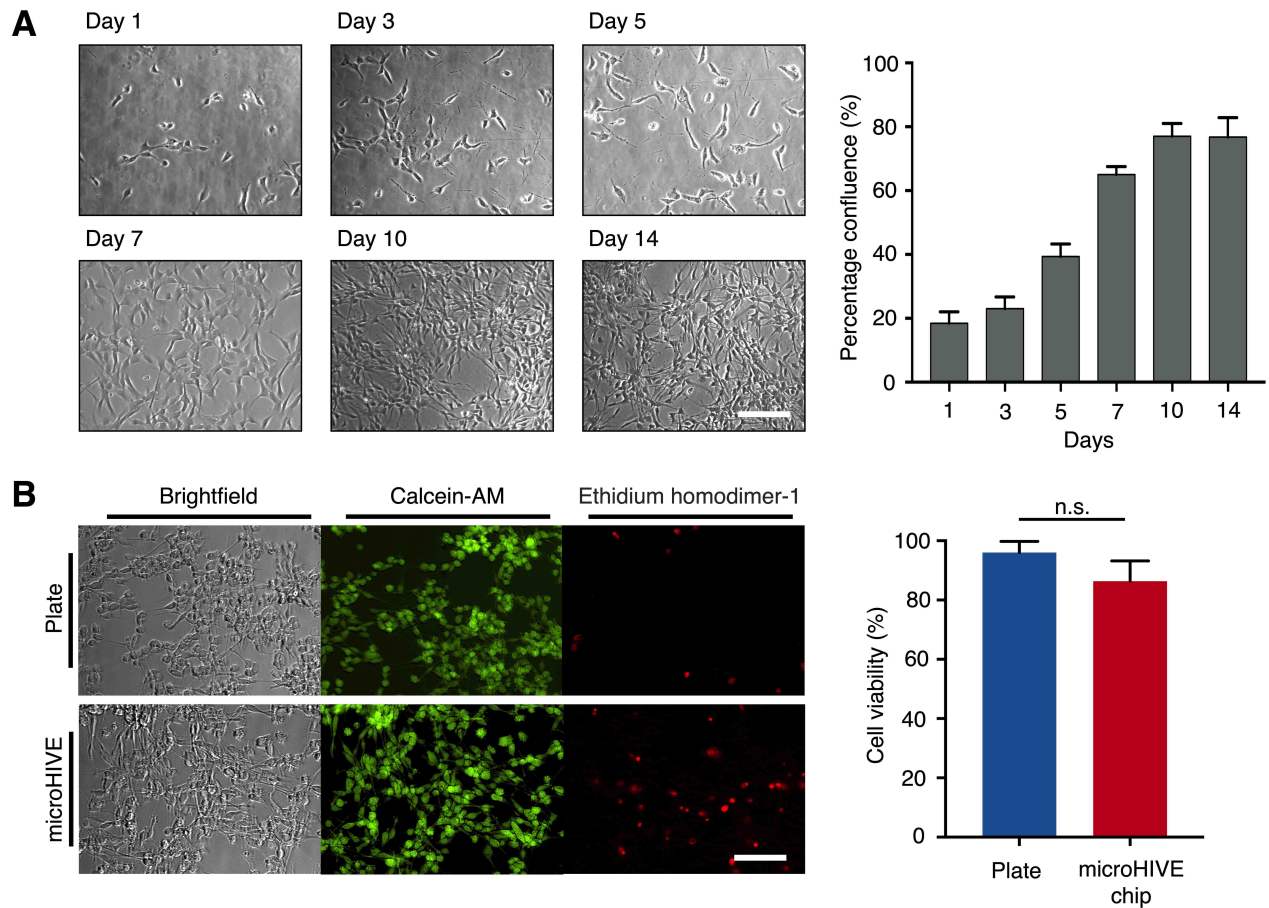


**Figure S10. Stem cell proliferation in the microHIVE platform.**

**(A)** Brightfield microscopy images of cells within the microHIVE culture chamber over 14 days (left). Image analysis was performed using ImageJ to determine the cellular percentage confluence (right). **(B)** Live/dead staining of cells cultured on gold-standard polystyrene plate and the microHIVE platform. Cells were stained with calcein-AM (green) and ethidium homodimer-1 (red) to determine the cellular viability. All scale bars indicate 100  $\mu$ m. (n.s. not significant, Student's *t*-test.)

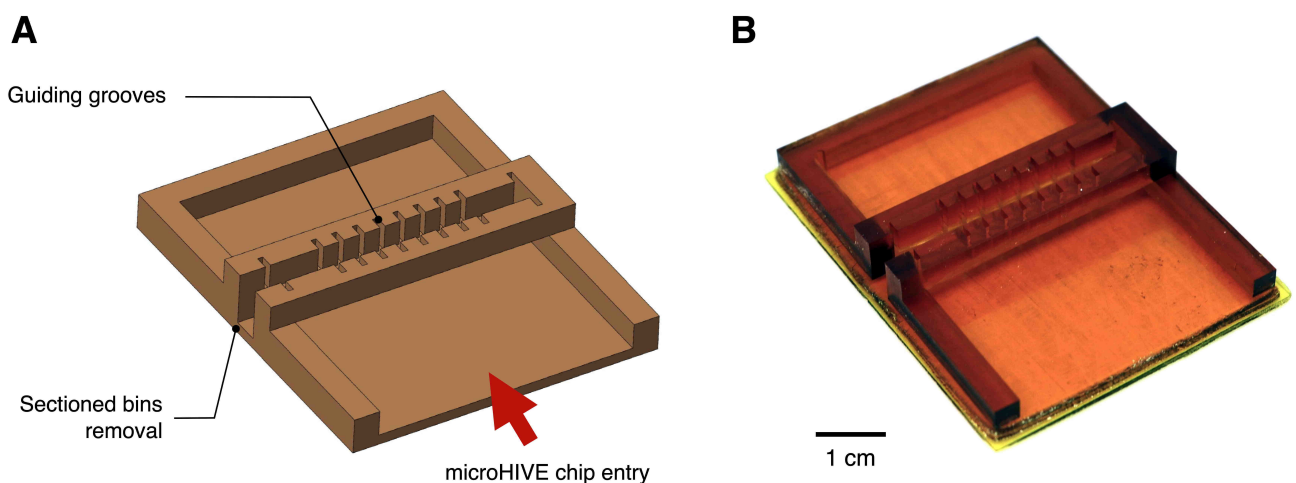


**Figure S11. Custom 3D-printed chip holder for sectioning of the microHIVE culture chamber.**

**(A)** 3D CAD model of the chip holder. The holder consists of guiding grooves for sectioning of the microHIVE culture chamber. **(B)** Photograph of the 3D-printed holder.

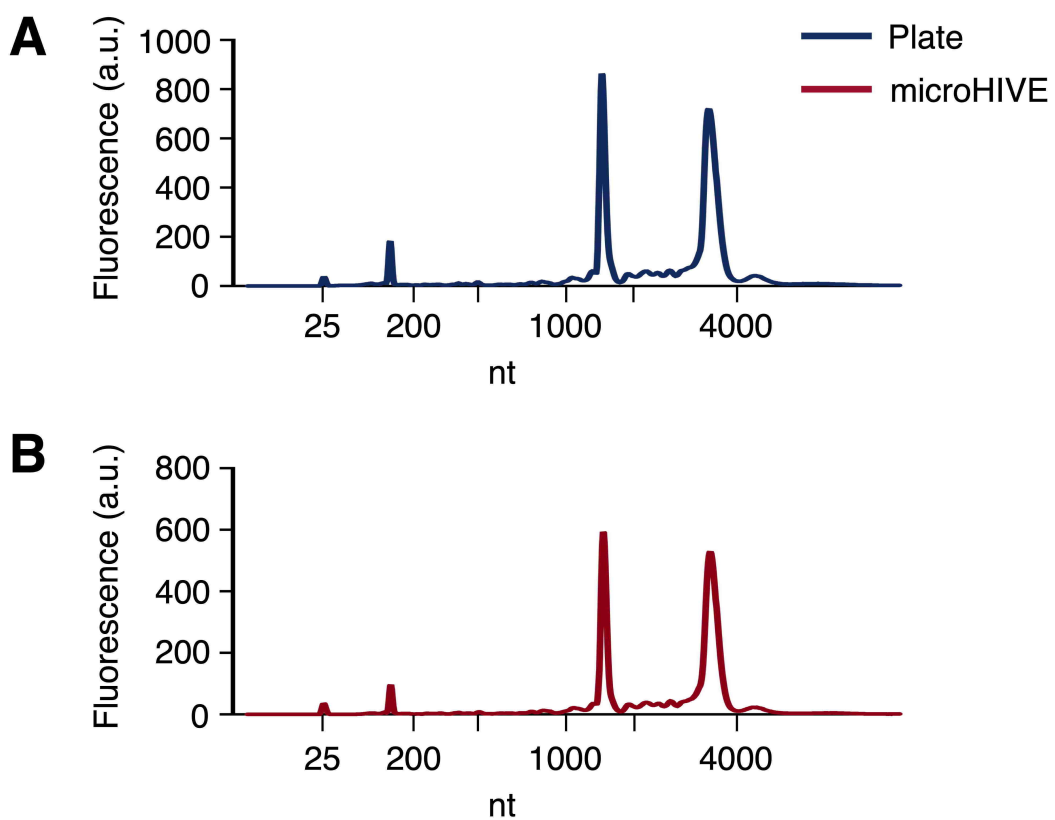


**Figure S12. Comparison of extracted RNA integrity.**

RNA samples were isolated from differentiated neuronal cultures, grown on **(A)** gold-standard polystyrene plate or **(B)** microHIVE culture section. For RNA extraction from the microHIVE section, the section was placed directly in lysis reagent and RNA was extracted from the lysate. All RNA samples were evaluated as bioanalyzer electropherograms for quality control.

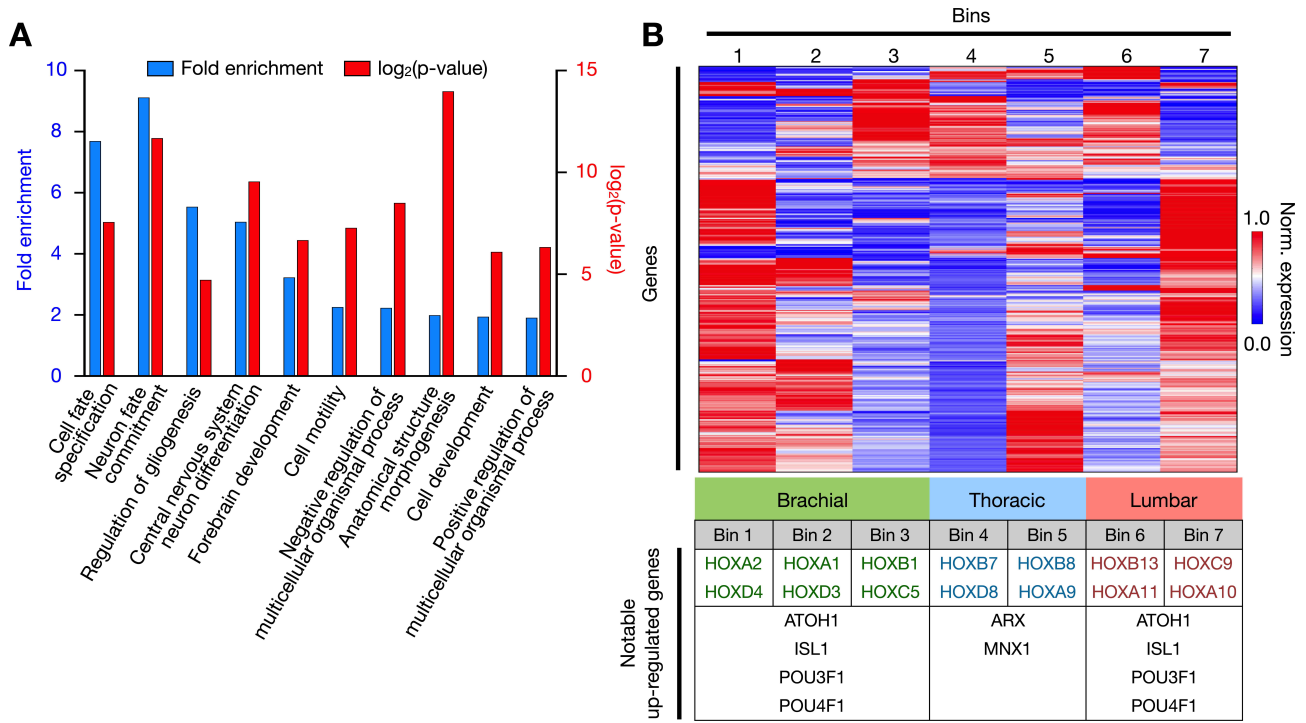


**Figure S13. Bin-based RNA sequencing analysis of microHIVE differentiation of spinal motor neurons.**

**(A)** Gene Ontology enrichment of differentially expressed genes. RNA sequencing analysis was performed on the microHIVE-derived cells. To verify the differentiation of iPSCs into spinal motor neurons, we conducted Gene Ontology enrichment for biological processes on the differentially expressed genes. The enriched biological processes are mostly neuronal or developmental-associated, supporting the successful differentiation into neurons. **(B)** Bin-based patterning of genes. Hierarchical clustering of the differentially expressed genes identified through RNA sequencing analysis was performed to demonstrate the patterning of upregulated and downregulated genes across the bins (top). All gene expression analyses were normalized to obtain FPKM values, and these were subsequently gene (row) normalized across all bins to compare respective gene expression trends in the form of a heat map. Several characteristic genes were identified to be upregulated across specific bins corresponding to the brachial, thoracic and lumbar regions of the spinal cord (bottom). In particular, the *HOX* genes showed progressive and characteristic signatures across the bins, while the thoracic bins had enriched expression of genes involved in spinal cord motor neuron development (e.g., ARX, MNX1) and the brachial and lumbar bins had enriched expression of transcription factors involved in neuron differentiation (e.g., ATOH1, ISL1, POU3F1, POU4F1).

**Table S1. Primers used for mRNA expression analysis.**

Characterization of cell identity		
Transcript	Forward Primer	Reverse Primer
NESTIN	CAGCGTTGGAACAGAGGTTGG	TGGCACAGGTGTCTCAAGGGTAG
SOX1	GCGGAAAGCGTTTCTTG	TAATCTGACTTCTCCTCCC
SMI32	AAGTTTATTATGGTTGAGTAGG	TGGTAGGAGGCAATGTCTGCC
ISL1	AAGGACAAGAAGCGAAGCAT	TTCCTGTCATCCCTGGATA

HOX genes list		
Transcript	Forward Primer	Reverse Primer
HOXA3	GATTTTAGACAGCTCATGAAACG	GGTTTGACACCCGTGAGG
HOXB4	CTGGATGCGCAAAGTTCAC	AGCGGTTGTAGTGAAATTCTT
HOXC4	ATCCCGCTGCCTCTACCT	CGAGCTCATGATCATTAATTCC
HOXC5	CCCGGGATGTACAGTCAGAA	GCCTGCTCCTCTTGATCTC
HOXA6	GCAGCGGATGAACTCCTG	GGTTGAAGTGGAACCTCTCTC
HOXA7	CTGGATGCGGTCTTCAGG	GGTAGCGGTTGAAGTGGAAC
HOXB7	CTGGATGCGAAGCTCAGG	CAGGTAGCGATTGTAGTGAAATTCT
HOXB8	CACAGCTCTCCCCCTGGA	CGCTTACGAGTCAGATAGGGATT
HOXC8	CATGTTCCATGGATGAGACC	GGTCTGATACCGGCTGTAAGTT
HOXD8	GTTTCCGTGGATGAGACCAC	TGGAAGCGACTGTAGGTTGT
HOXA9	CCCCATCGATCCCAATAA	CACCGCTTTCCGAGTG
HOXC9	GCAGCAAGCACAAAGAGGA	CGTCTGGTACTGGTAGGG
HOXD9	AGCAGCAACTGACCCAAA	CGGGTGAGGTACATGTTGAA
HOXD10	CTGAGGTCTCCGTGTCCAGT	GCTGGTTGGGTATCAGACTTG
HOXC11	AGGCTGAGGAGGAGAACACA	TAAGGGCAGCGCTTCTTG

Housekeeping genes list		
Transcript	Forward Primer	Reverse Primer
ACTINB	CCA ACC GCG AGA AGA TGA	CCA GAG GCG TAC AGG GAT AG
GAPDH	AGC CAC ATC GCT CAG ACA C	GCC CAA TAC GAC CAA ATC C

**Table S2. Primary antibodies used for immunofluorescence staining.**

Primary antibodies for immunofluorescence		
Antibody	Description	Manufacturer
Nestin	Nestin is a class VI intermediate filament protein that is expressed in stem cells of the central nervous system but not in mature CNS cells. Nestin expression is used extensively as a marker for CNS stem cells.	Abcam, ab22035
SOX1	SOX1 maintains neural cells in an undifferentiated state and has been used as a marker for neural stem cells.	Abcam, ab87775
SMI-32	SMI-32 is a non-phosphorylated neurofilament H. It is used as a marker for mature neuronal cell bodies, dendrites, and some thick axons in the central and peripheral nervous systems.	Calbiochem, NE-1023
ISL1	ISL1 is a member of a family of homeodomain containing transcription factors. It is an early marker for motor neuron differentiation.	Abcam, ab109518
HOXB4	HOXB4 is a sequence-specific transcription factor which is part of a developmental regulatory system that provides cells with specific positional identities (i.e., brachial region) on the rostral-caudal axis.	Abcam, ab133521
HOXC8	HOXC8 is a sequence-specific transcription factor which is part of a developmental regulatory system that provides cells with specific positional identities (i.e., thoracic region) on the rostral-caudal axis.	Abcam, ab86236
MAP2	MAP2 belongs to the microtubule-associated protein family and is involved in microtubule assembly, which is an essential step in neuritogenesis. MAP2 is used as a microtubule formation in motor neurons.	Abcam, ab11267
OCT4	OCT4 is a transcription factor that forms a trimeric complex with SOX2 on DNA and controls the expression of a number of genes involved in embryonic development. OCT4 is used as a marker for early embryogenesis and for embryonic stem cell pluripotency.	Santa Cruz, sc-9081
SOX2	SOX2 is a transcription factor that forms a trimeric complex with OCT4 on DNA and controls the expression of a number of genes involved in embryonic development. SOX2 is also used as a marker for early embryogenesis and for embryonic stem cell pluripotency.	Santa Cruz, sc-17320